Mid-infrared spectroscopy of molecular ions in helium nanodroplets

Xiaohang Zhang,[1] Nils B. Brauer,[1] Giel Berden,[2] Anouk M. Rijs,[2,a)] and Marcel Drabbels[1,b)]
[1]*Laboratoire de Chimie Physique Moléculaire, Ecole Polytechnique Fédérale de Lausanne (EPFL), CH-1015 Lausanne, Switzerland*
[2]*FOM Institute for Plasma Physics Rijnhuizen, Edisonbaan 14, 3439 MN Nieuwegein, The Netherlands*

(Received 12 November 2011; accepted 31 December 2011; published online 24 January 2012)

High resolution IR spectra of aniline, styrene, and 1,1-diphenylethylene cations embedded in superfluid helium nanodroplets have been recorded in the 300–1700 cm^{-1} range using a free-electron laser as radiation source. Comparison of the spectra with available gas phase data reveals that the helium environment induces no significant matrix shift nor leads to an observable line broadening of the resonances. In addition, the IR spectra have provided new and improved vibrational transition frequencies for the cations investigated, as well as for neutral aniline and styrene. Indications have been found that the ions desolvate from the droplets after excitation by a non-evaporative process in which they are ejected from the helium droplets. The kinetic energy of the ejected ions is found to be ion specific and to depend only weakly on the excitation energy. © *2012 American Institute of Physics*. [doi:10.1063/1.3678011]

I. INTRODUCTION

It is well established that helium nanodroplets due to their low temperature and weak interaction with embedded species, provide an almost ideal spectroscopic matrix for molecules.[1–4] The advantages of helium nanodroplet spectroscopy are exemplified in several studies where structural information of molecules or complexes could be obtained.[5–8] Whereas helium nanodroplet spectroscopy has become a standard technique for neutral species, it is only recently that helium droplets have been doped directly by molecular ions[9] and that the first vibrational[10] and electronic[11] spectra of ions in helium droplets have been recorded. These first studies revealed that despite the fact that ions interact much more strongly with helium than neutrals, the effect of the helium environment on the spectra, in terms of matrix shift and line broadening, is quite similar for ions and neutrals. These studies furthermore indicated that the dynamical evolution of the system after excitation of the embedded chromophore proceeds differently for ions than for neutrals. According to the generally accepted model, following the energy transfer from the excited chromophore to the helium bath, the heated droplet cools by the evaporation of individual helium atoms from its surface.[12–14] The net result of the absorption of a photon by the chromophore is a reduction of the helium droplet size. In contrast, it was found that the dynamics following the vibrational excitation of an ion is governed by a non-thermal process in which the ion is ejected from the helium droplet.[10] Although some insight into the process could be obtained, most of the details are still unknown.

The initial spectroscopic experiments on ion-doped helium nanodroplets were performed on the aniline cation that was excited via high-frequency NH-stretch vibrations.[10] Since only a single system was investigated, it is not evident that the conclusions of that study can be generalized. In the present work, we extend the study to other ionic systems and to low frequency vibrations. The experiments have been performed at the free-electron laser based IR facility FELIX (Free Electron Laser for Infrared eXperiments) located at the FOM Institute Rijnhuizen in the Netherlands.[15] The wide tuning range of FELIX allows the excitation of a large variety of vibrations. The systems investigated range from simple aromatics, to amino acids, to fullerenes. Here, we report on the results for the aromatic systems: aniline, styrene, and 1,1-diphenylethylene (DPE). These species are widely used for the production of polymers with robust properties and are thought to be representative of a large class of molecular ions. The vibrational energy levels of these cations have been extensively characterized using zero kinetic energy (ZEKE) spectroscopy and related techniques.[16–22] Furthermore, IR spectra of the aniline cation have been recorded by matrix isolation spectroscopy and the argon tagging technique.[23,24] Comparison of spectra obtained in helium droplets to these data provides a means to determine the effect of the helium environment on the vibrational energy levels. At the same time the spectra provide new and improved vibrational frequencies for these cations. To verify whether the ejection of ions from the droplets after vibrational excitation is a universal process, time-of-flight mass spectra have been recorded and the speed distributions of the desolvated ions have been determined at different excitation energies for each of the three molecules investigated.[10]

II. EXPERIMENTAL SETUP

The experimental setup has been described in detail before.[25,26] Briefly, helium droplets consisting on average of 1000–20 000 helium atoms are produced by expanding high

a)Present address: Radboud University Nijmegen, Institute for Molecules and Materials, Toernooiveld 7, 6525 ED Nijmegen, The Netherlands.
b)Author to whom correspondence should be addressed. Electronic mail: Marcel.Drabbels@epfl.ch.

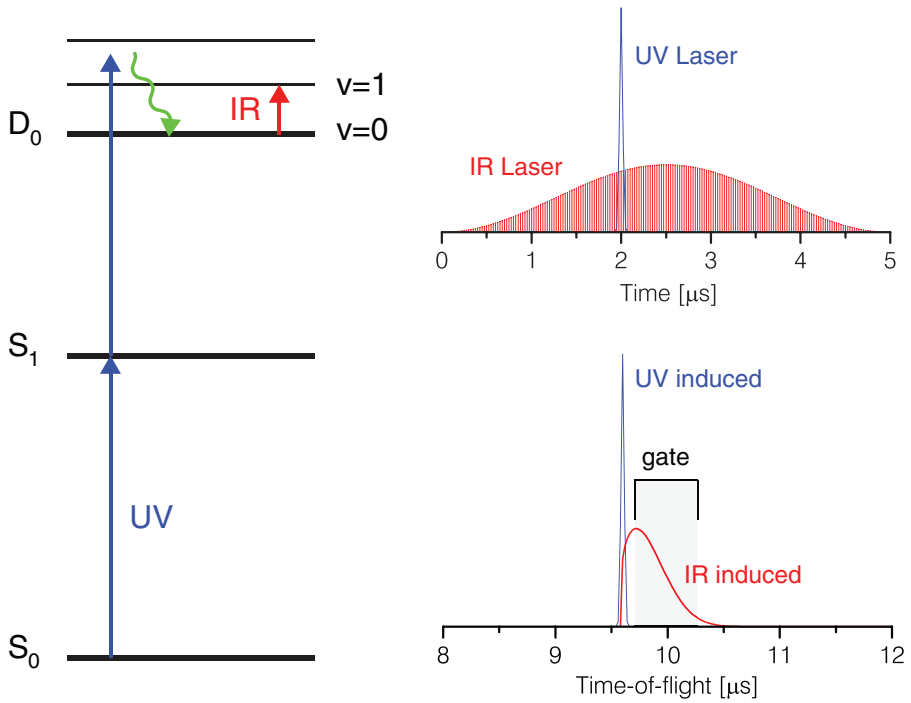

FIG. 1. Energy level diagram indicating the resonant ionization scheme used to record IR spectra of ions (left). Timing diagram indicating temporal structure and timing of the ionization (UV) and excitation (IR) laser pulses (upper right). Schematic time-of-flight spectrum indicating the contributions of bare ions produced by the UV ionization of neutral molecules and those resulting from the IR excitation of ions in helium droplets.

purity helium gas at a stagnation pressure of 30 bars into vacuum through a 5 μm nozzle that is cooled to temperatures in the range of 11–22 K.[27] The helium droplets pick up molecules by inelastic collisions, as they pass through a vapor of the molecule of interest. The vapor pressure is adjusted to maximize the pickup of a single molecule. Via a differential pumping stage, the doped helium droplets enter a velocity map imaging spectrometer mounted perpendicular to the droplet beam axis. At the center of the spectrometer the embedded molecules are ionized via a two-photon absorption process. In the case of aniline, the molecules are resonantly ionized via the $S_1 \leftarrow S_0$ band origin at 34 100 cm^{-1} by the weakly focused output (2 mJ/pulse) of a pulsed dye laser system operated at a repetition rate of 10 Hz.[28] All other molecules investigated are non-resonantly ionized by focusing the frequency-quadrupled output of a Nd:YAG laser (8 mJ/pulse at 266 nm) by a 40 cm focal length lens onto the droplet beam. The created ions, which relax on a subnanosecond time scale to the vibrational ground state in the helium droplets,[10] are exposed to infrared radiation in the energy range of 300–1700 cm^{-1} provided by the FELIX free-electron laser.[15] FELIX is operated at a 10 Hz repetition rate and provides macropulses with $\sim$5 μs duration having a pulse energy ranging from 30 to 60 mJ. Each macropulse consists of a train of micropulses of picosecond duration that are separated by 1 ns. The bandwidth of the infrared radiation is 0.25%–0.4% of the central frequency (FWHM). The IR light is focused into the imaging setup by a concave mirror with 5 m focal length, yielding a spot size of $\sim$1 mm diameter at the droplet beam. The intensity of the light can be reduced by fixed-value attenuators, if required. The IR and UV laser beams propagate orthogonal to both the droplet beam and the axis of the imaging setup, while their polarization is parallel to the molecular beam axis. In order to have the ions interact with IR micropulses of highest intensity, the UV laser beam is fired 2 μs after the onset of the IR pulse. A schematic diagram of the excitation scheme and the timing of the lasers can be found in Fig. 1.

The ions created by the UV and IR radiation are accelerated towards a position sensitive detector consisting of a set of microchannel plates coupled to a phosphor screen. The electrical signal from the phosphor screen is fed into a multichannel scaler which allows recording ion time-of-flight mass spectra. The light emitted by the phosphor screen is imaged onto a high-resolution CCD camera that is read out every laser shot. The individual images are analyzed online and the centroids of the ion impacts are determined. The velocity distributions of the ions are determined by performing an inverse Abel transform on the image constructed from the accumulated centroids at a given excitation frequency. Vibrational spectra of the ions are recorded by monitoring the number of parent ion impacts on the detector as a function of the IR frequency. As mentioned above, in a first step neutral molecules embedded in helium droplets are ionized by UV radiation. This ionization process not only leads to the formation of ion-containing helium droplets but also results in the non-thermal ejection of ions from the helium droplets.[10] In order to discriminate between these ions and those that result from the excitation by the IR radiation, a gating voltage is applied to the front of the detector. The detection gate is set directly after the ion signal resulting from the UV ionization and has a width of 650 ns, see Fig. 1. It was experimentally found that these settings resulted in spectra with the highest signal-to-noise ratio.

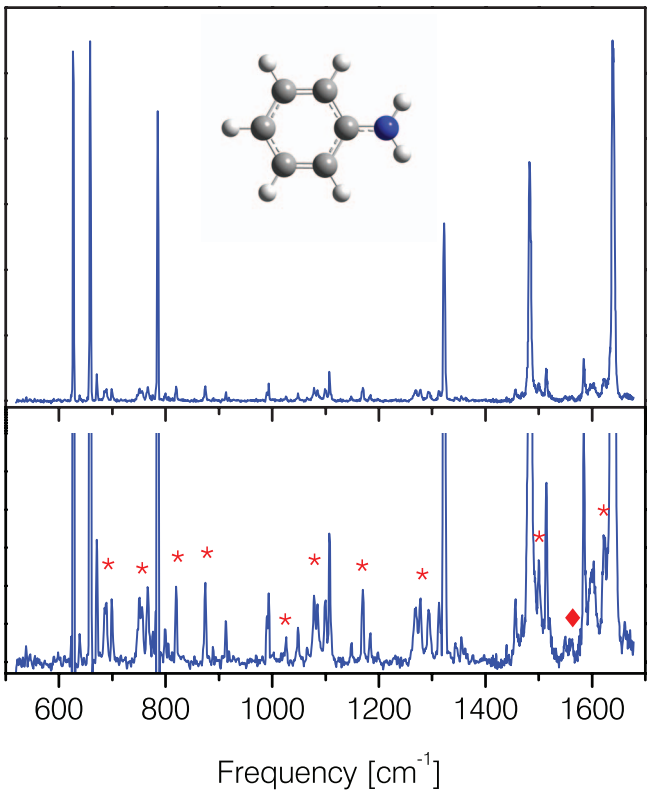

FIG. 2. (Upper panel) IR excitation spectrum of aniline ions in helium droplets consisting on average of 2700 atoms. (Lower panel) Expanded view of the same spectrum. The peaks denoted by an asterisk correspond to transitions of neutral aniline molecules in helium droplets, while the peak denoted by a diamond corresponds to the aniline$_2^+$ complex.

III. RESULTS AND DISCUSSION

A. Spectroscopy

1. Aniline

The spectroscopy of the aniline cation is well characterized and consequently it offers a means to investigate in a systematic way the effect of the helium environment on the spectra.[16–18,23,24] The excitation spectrum of aniline radical cations in helium nanodroplets recorded in the mid-IR, 500–1700 cm^{-1}, is shown in Fig. 2. The helium droplets used to record this spectrum are estimated to consist on average of 2700 helium atoms before pickup of the molecules. Identical spectra have been recorded for both smaller and larger droplets. The spectrum in Fig. 2 which has been corrected linearly for the variation in IR laser intensity shows a series of strong resonances. The transition frequencies of the resonances have been determined with an accuracy of 0.35%—corresponding to 2 cm^{-1} at the low and 6 cm^{-1} at the high frequency range of the spectrum—and are listed in Table I. Based on previous experimental and theoretical work,[16–18,23,24,29] the main spectral features are readily assigned to fundamental transitions with the exception of the band at 1327 cm^{-1}. This feature has been assigned to the overtone transition of the inversion mode, I_0^2, which is observed at 1323–1325 cm^{-1} in the gas phase.[16,17] The fundamental transition of this vibration is found at 659 cm^{-1}, which agrees very well with the gas phase transition frequency of 656–660 cm^{-1}.[16–18] Not only the inversion mode agrees well with the gas phase data, but also the transition frequencies of other vibrations match the gas phase data within the accuracy of the experiment, see Table I. It is interesting to note that while the agreement of the helium droplet data with the gas phase data is almost perfect, the agreement with the aniline$^+$-Ar data is less satisfactory.[24] Especially those vibrations that involve a large motion of the amino-group hydrogen atoms reveal a noticeable difference in transition frequencies. We attribute this discrepancy to the fact that the argon atom affects the motion of the hydrogen atoms, leading to a redshift of the vibrational transition frequencies.[30,31] Apparently, the more abundant but lighter helium atoms surrounding the ion have a much smaller effect on the transition frequencies.

TABLE I. Comparison of the vibrational transition frequencies (cm^{-1}) of the aniline radical cation.

Helium droplets	Gas phase[a]	Argon tagging[b]
628	629/628[c]	622
659	658/656[d]/ 660[c]	652
788		785
890	889	
915		913
995	996/993[d]	993
1110		1107
1152	1153	
1187	1188/1193[c]	
1327	1325/1323[d]	1317
1488		1483
1520		1515
1591	1594/1593[d]	1583
1645		1635

[a]Reference 16.
[b]Reference 24.
[c]Reference 18.
[d]Reference 17.

The resonances observed in the helium droplet spectra are well described by a Gaussian line profile. The widths of the transitions (FWHM) increase linearly with excitation frequency from 1.5 cm^{-1} to 4.5 cm^{-1}, which is consistent with the 0.25% relative bandwidth of FELIX. From this, we deduce that the intrinsic width of the resonances is at most 1 cm^{-1}. Taking into account that the rotational band contour contributes 0.4 cm^{-1} to the linewidth of the resonances,[10] we conclude that the interaction of the ion with the helium does not lead to a substantial line broadening.

The observations discussed can be summarized in the following conclusion: thus, although ions interact much stronger than neutrals with helium,[32–34] the effect of the helium environment on the IR spectra is similar in terms of matrix shift and line broadening. In this respect, helium nanodroplets can also be considered an ideal spectroscopic matrix for ions.

In addition to the strong transitions discussed above, the spectrum also reveals many weak transitions. Most of these are found to correspond to fundamental bands of neutral aniline. The observation of transitions of neutral aniline can be attributed to the particular pulse structure of FELIX and the detection method used. Since the neutral aniline molecules are exposed to the IR radiation during ~2 μs prior to

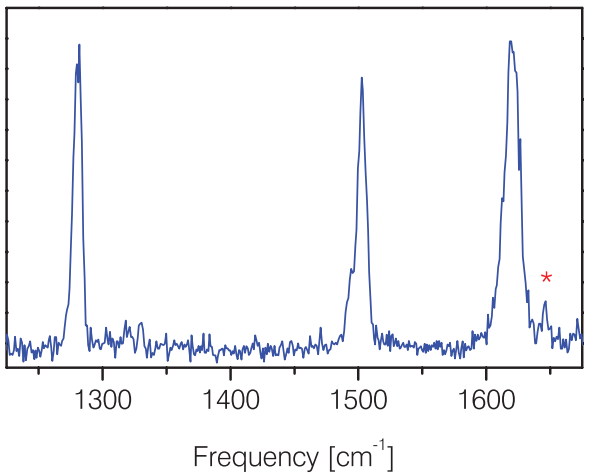

FIG. 3. IR excitation spectrum of neutral aniline molecules in helium droplets. The transition denoted by an asterisk belongs to the aniline cation.

ionization by the UV laser pulse, see Fig. 1, the vibrations of the aniline neutral can readily be excited. The vibrational energy is quickly transferred to the helium droplet leading to the evaporation of helium atoms from its surface. The resulting size reduction of the helium droplets is then reflected as an increase in the photoionization probability of the embedded neutral molecule.[13] Even though the detector is gated to minimize the contribution of ions created by the ionization process, it cannot be totally eliminated. As a result, the recorded spectrum will also contain contributions from neutral aniline. This hypothesis is confirmed by the spectrum shown in Fig. 3 that has been recorded by setting the detection gate as to maximize the neutral aniline signal. In this case, the contribution of aniline cations to the spectrum is very small, only the strong transition at 1645 cm^{-1} can be observed. The transition frequencies of neutral aniline as determined in the present experiment are reported in Table II and show good agreement with available gas phase and matrix data.[23,35,36] Since the gas phase data reported in the literature have a limited accuracy, high resolution ion-dip double-resonance spectra of cold aniline molecules in a molecular beam have been recorded (see supplementary material for details[37]) to allow for a more precise comparison. Inspection of Table II reveals an excellent agreement between the helium droplet data and the new high resolution gas phase data. This observation is in line with previous investigations which have demonstrated that the vibrational spectra of neutral molecules in helium droplets reveal only a minor matrix shift.[1,4] At low frequency, also a good agreement with the aniline-Ar data is found.[24] However, at higher energies the aniline-Ar transition frequencies are systematically lower than those found in the present and other studies.[23,35] The reason for this difference remains unclear.

TABLE II. Comparison of the vibrational transition frequencies (cm^{-1}) of the aniline molecule.

Helium droplets	Gas phase[a]	Gas phase[b]	Argon tagging[c]	Argon matrix[d]
688	690	687	688	688–690
754	740–760	752	755	752–757
821	820–830	822	822	822
875	874	876	867	875–877
1028	1028	1027		1028–1029
1087	1077–1090	1088	1084	1085
1173	1166–1180			1175–1176
1273	1270–1287	1275		
1282	1270–1287		1277	1280–1284
1503	1504.297[e]	1502	1496	1503–1505
1622	1611–1628	1622	1610	1618–1624

[a]Reference 35.
[b]This work, see supplementary material for details.[37]
[c]Reference 24.
[d]Reference 23.
[e]Reference 36.

2. Aniline dimer

Inspection of the spectrum reported in Fig. 2 reveals two weak transitions at about 1565 cm^{-1} that cannot be assigned to transitions of either the aniline neutral or its cation. Under the conditions used to record the spectrum, an appreciable fraction of the helium droplets is expected to contain two or even more aniline molecules. These molecules will form complexes in the helium droplets which will be ionized by the UV radiation.[10,38] Even though the spectrum in Fig. 2 has been recorded by gating the detector at the aniline monomer mass range, the cationic aniline complexes might still contribute via IR multiphoton dissociation.[39] Indeed, the spectra shown in Fig. 4, which have been recorded by using a

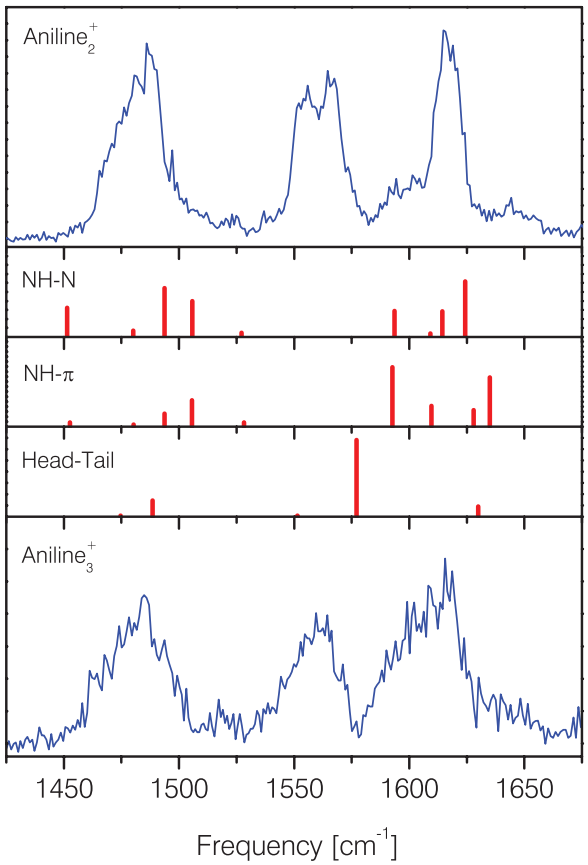

FIG. 4. IR excitation spectrum of $aniline_2^+$ and $aniline_3^+$ complexes in helium droplets and the calculated spectrum of $aniline_2^+$ for the NH-N, NH-π, and head-to-tail geometries, see text for details.

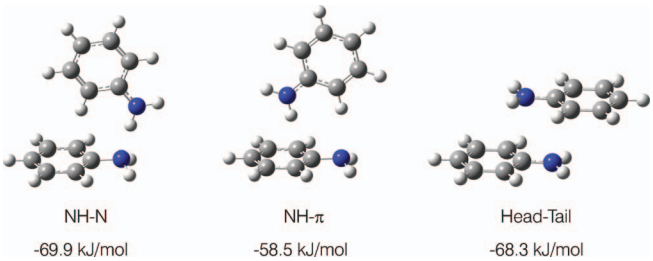

FIG. 5. Structures of the aniline$_2^+$ cation calculated by DFT at the B3LYP/6-311^{++}G(*df*,*pd*) level of theory.

UV frequency of 34 000 cm^{-1} as to maximize the ionization probability for aniline complexes[10] and by gating the detector in the aniline dimer and trimer mass ranges, show similar spectroscopic features in the 1565 cm^{-1} frequency range. The spectrum recorded at the dimer mass reveals two intense transitions at 1559 and 1571 cm^{-1} in addition to transitions at 1488 and 1620 cm^{-1}. In the spectrum of the trimer the two closely spaced lines have merged into a single peak. Whereas the transitions at 1488 and 1620 cm^{-1} have counterparts in the spectrum of the ionic and neutral monomers, the transitions at about 1565 cm^{-1} appear to be related to a collective vibrational motion of the complex.

Theoretical calculations and gas phase experiments both indicate that the lowest energy conformer of the aniline$_2^+$ dimer corresponds to a NH–N hydrogen bonded structure.[40–42] The NH-π bounded conformer has been calculated to be ~10 kJ/mol higher in energy.[41] The structures of these complexes are shown in Fig. 5. The vibrational frequencies of these two conformers have been calculated by density functional theory (DFT) at the B3LYP/6-311^{++}G(*df*,*pd*) level using the GAUSSIAN09 suite of programs.[43] The calculated harmonic frequencies have been scaled by 0.983 to yield the spectra plotted in Fig. 4.[29] In both theoretical spectra the transitions around 1565 cm^{-1} are markedly absent. This suggests either that the theoretical method used is not suitable for the system at hand, or that the structure of the aniline$_2^+$ dimer is different in helium droplets than in the gas phase. This latter option is not unfeasible in view of the high cooling rate and low temperature of helium droplets. It is very well possible that following the ionization of the neutral aniline dimer, the created aniline$_2^+$ complex gets trapped in a local minimum on the potential energy surface that resembles the structure of the neutral complex. It should be noted that stabilization by the helium environment of configurations not corresponding to the minimum energy has been observed before.[5,6,44] The most stable structure of the neutral aniline dimer has been found to correspond to a sandwiched head-to-tail arrangement with double NH$_2$–π bonds and almost equivalent aniline monomers.[45,46] Using this structure as input for the DFT calculations we find a local minimum with a similar sandwiched head-to-tail structure for the aniline$_2^+$ ionic complex, see Fig. 5. This structure is found to be only 1.6 kJ/mol higher in energy than the NH–N hydrogen bonded system, and 9.8 kJ/mol lower in energy than the NH-π bounded structure. The IR spectrum corresponding to the head-to-tail configuration is shown in Fig. 4 and is characterized by a strong transition at 1577 cm^{-1}, in addition to transitions at 1488 and 1623 cm^{-1}. The agreement with experiment is significantly better for this conformation compared to the HN-H and NH-π bounded systems discussed above. However, it should be noted that the calculations do not reproduce the splitting of the band at 1565 cm^{-1}. This splitting could be related to a breaking of the symmetry by the helium environment. The overall good agreement between the theoretical and experimental spectrum for the head-to-tail sandwich structure leads us to conclude that the structure of the aniline dimer cation in helium droplets does not correspond to the minimum energy gas phase structure, but rather resembles the structure of its neutral aniline dimer precursor. We would like to point out that the sandwich structure is compatible with the spectrum of the aniline$_2^+$ dimer recorded in the 3 μm region in our previous study.[10] As for the aniline trimer, the strong resemblance of its spectrum to that of the dimer strongly suggests that the cationic dimer acts as a core upon which the trimer structure is built. The present data, however, are too limited to confirm this hypothesis.

3. Styrene

In addition to the aniline cation, we have successfully applied helium droplet isolation spectroscopy to a variety of other molecular ions having different functional groups and sizes. Figure 6 shows the IR spectrum of styrene cations in helium droplets recorded using non-resonant ionization of the neutral styrene molecule. The spectrum exhibits a similar signal-to-noise ratio as that of aniline, indicating that non-resonant ionization by 266 nm is a viable and efficient method to produce ions in helium droplets. The transition frequencies of the observed resonances are reported in Table III. For comparison, we also list the vibrational frequencies for this system as determined by ZEKE spectroscopy.[20,21] To aid the assignment of the spectrum, DFT calculations have been performed

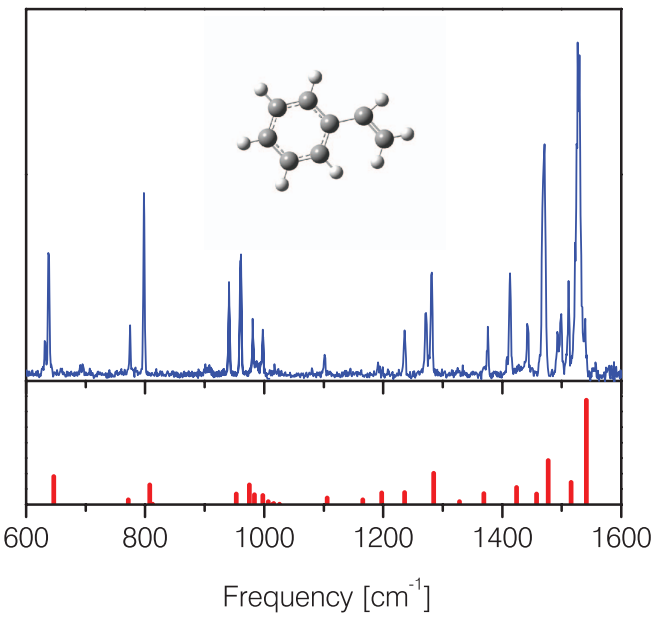

FIG. 6. IR excitation spectrum of the styrene cation in helium droplets (upper panel) and the theoretical spectrum based on DFT calculations at the B3LYP\6-311^{++}G(*df*,*pd*) level of theory (lower panel).

TABLE III. Comparison of the observed vibrational transition frequencies of styrene radical cation and the scaled theoretical harmonic frequencies (cm^{-1}) calculated using DFT at the B3LYP\6-311^{++}G(*df*,*pd*) level of theory. Also indicated are the calculated intensities (km/mol).

Helium droplets	Gas phase	Theory	Intensity
639		647	45.1
776	776[a]/780[b]	772	7.5
799		808	31.5
942		953	17.2
962		975	31.8
982	982[b]	983	15.6
999		997	14.4
1103		1106	10.5
1193		1198	18.8
1238	1241[a]	1236	19.1
1274			
1283		1285	50.3
1380		1369	17.4
1416		1424	27.8
1446		1458	16.8
1473		1477	70.8
1514		1515	35.9
1532		1541	168.1

[a]Reference 21.
[b]Reference 20.

at the B3LYP/6-311^{++}G(*df*,*pd*) level of theory. The calculated harmonic frequencies for the styrene cation have been scaled by 0.983 to yield the frequencies reported in Table III.[29] A complete list of calculated frequencies can be found in the supplementary material.[37]

The transition observed at 776 cm^{-1} is readily assigned to the γ_{25} vibrational mode based on the excellent agreement with the gas phase data which place this band at 776–780 cm^{-1} (Refs. 20 and 21) and the calculated frequency of 772 cm^{-1}. The same level of agreement is found for the transition at 982 cm^{-1}, corresponding to the benzene vibrational mode 12.[47] Although the agreement with the gas phase data is not as good for the transition at 1238 cm^{-1}, it is still well within the estimated accuracies by which these frequencies have been determined. The good agreement between the gas phase and helium droplet data confirms our conclusion that the helium environment induces an almost negligible matrix shift. By comparing the experimentally observed spectrum to the theoretical spectrum of the styrene cation, see Fig. 6, it is straightforward to assign most of the observed resonances. Of the unassigned transitions, all except one can be attributed to vibrational transitions of neutral styrene. Analogous to aniline, their appearance in the experimental spectrum is caused by the vibrational excitation of the neutral molecules prior to the ionization by the UV light. The transition frequencies for neutral styrene which are reported in Table IV, all agree well with gas phase data. We tentatively assign the remaining unassigned transition at 1274 cm^{-1} to the overtone of the benzene mode 4 whose fundamental band is observed at 639 cm^{-1}.

4. 1,1-Diphenylethylene

As final example we present here in Fig. 7 the IR spectrum of the DPE cation in helium droplets. Since this molecule has many low frequency vibrational modes, the frequency range has been extended to cover the interval from 300–1700 cm^{-1}. The frequencies of the observed transitions are listed in Table V. Comparison with the gas phase data is only possible for the transition at 422 cm^{-1} which is located at 423 cm^{-1} in the free ion.[22] The good agreement between these frequencies indicates once more that the helium induces a negligible matrix shift. Table V also reports the results of DFT calculations performed at the B3LYP/6-311^{++}G(*df*,*pd*) level of theory. Analogous to neutral diphenylethylene, the calculations on the cation indicate that the coupling of the two phenyl groups gives rise to the appearance of pairs of closely

TABLE IV. Comparison of the observed vibrational transition frequencies (cm^{-1}) of neutral styrene in helium droplets and in the gas phase.

Helium droplets	Gas phase[a]
695	695
906	905
992	990
1500	1497

[a]Reference 52.

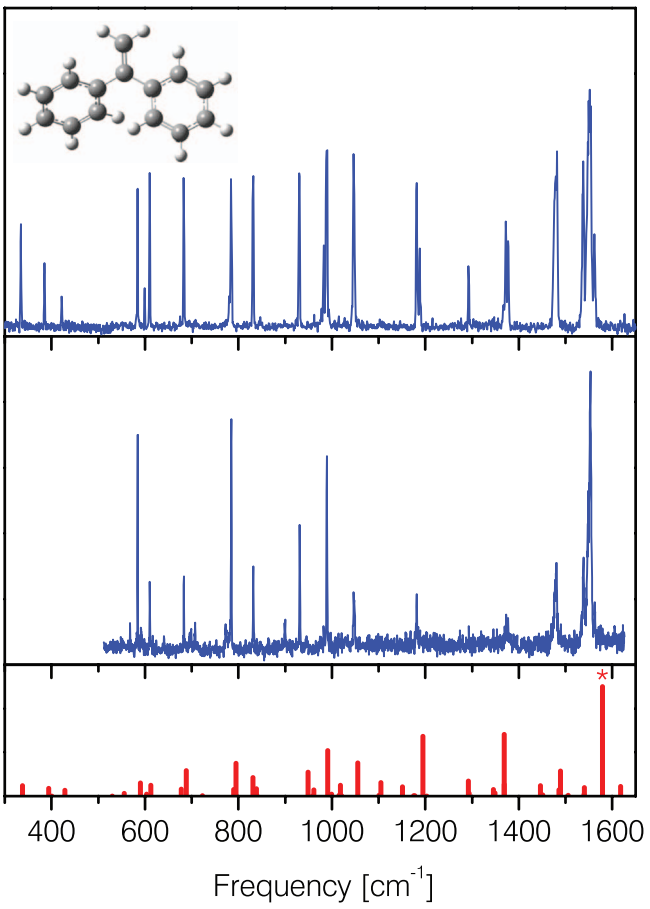

FIG. 7. (Upper panel) IR excitation spectrum of 1,1-diphenylethylene cations in helium droplets. (Middle panel) The same spectrum recorded with a factor two reduced IR intensity. (Lower panel) Theoretical spectrum of the 1,1-diphenylethylene radical cation based on DFT B3LYP\6-311^{++}G(*df*,*pd*) calculations. The intensity of the strongest transition at 1086 cm^{-1}, denoted by an asterisk, has been reduced by a factor 4 for a better comparison with the experimental spectra.

TABLE V. Comparison of the experimental vibrational transition frequencies of the 1,1-diphenylethylene radical cation in helium droplets with the scaled harmonic frequencies (cm^{-1}) calculated using DFT at the B3LYP\6-311^{++}G(*df,pd*) level of theory. Also indicated are the calculated transition intensities (km/mol).

Helium droplets	Theory	Intensity
334	338	23.4
385	394	18.0
422	429	13.6
584	590	30.0
610	613	24.5
683	689	57.7
785	795	74.7
831	831	42.1
930	949	54.4
989	991	103.6
1047	1056	76.1
1181	1194	136.5
1293	1292	34.6
1372	1369	140.4
1479	1489	56.9
1551	1579	1000.1

spaced bands for each fundamental vibrational mode.[48] A complete list of the calculated frequencies can be found in the supplementary material.[37] A comparison of the experimental and calculated spectra shown in Fig. 7 reveals that the calculations reproduce the transition frequencies fairly well. The spectrum shown in the upper panel of Fig. 7 has been recorded using the maximum IR intensity. The intensities of the transitions are all very similar and most of them do not match the calculated intensities. This indicates that the transitions are saturated by the high intensity of the IR light. The spectrum recorded using a factor of two reduced IR intensity shown in the middle panel of Fig. 7 reveals a better agreement with the calculations, although some discrepancies still remain. Interestingly, the intensity of some of the transitions, like the one at 1047 cm^{-1}, is reduced by a factor of almost four. It is unlikely that this is due to power variations, even though the spectra have been recorded at different days. The almost quadratic power dependence of the transition intensity most likely indicates that the ion absorbs multiple IR photons before being detected. This is certainly not unfeasible in view of the particular pulse structure of FELIX, which consists of micropulses separated by 1 ns, and the fast, sub-nanosecond vibrational relaxation induced by the helium.[28,49–51] It is unclear why saturation of the transitions is only observed for the DPE cation and not for the other systems. The calculated absorption cross sections for the vibrational transitions of the DPE cation are similar to those of the other ions reported here. Unfortunately, a systematic study of the power dependence of the transition intensities could not be performed in the limited beam time at the FELIX facility.

B. Desolvation mechanism

In our previous study, it was concluded that the desolvation of aniline cations that had been excited via the NH-stretch vibration is governed by non-thermal processes that lead to

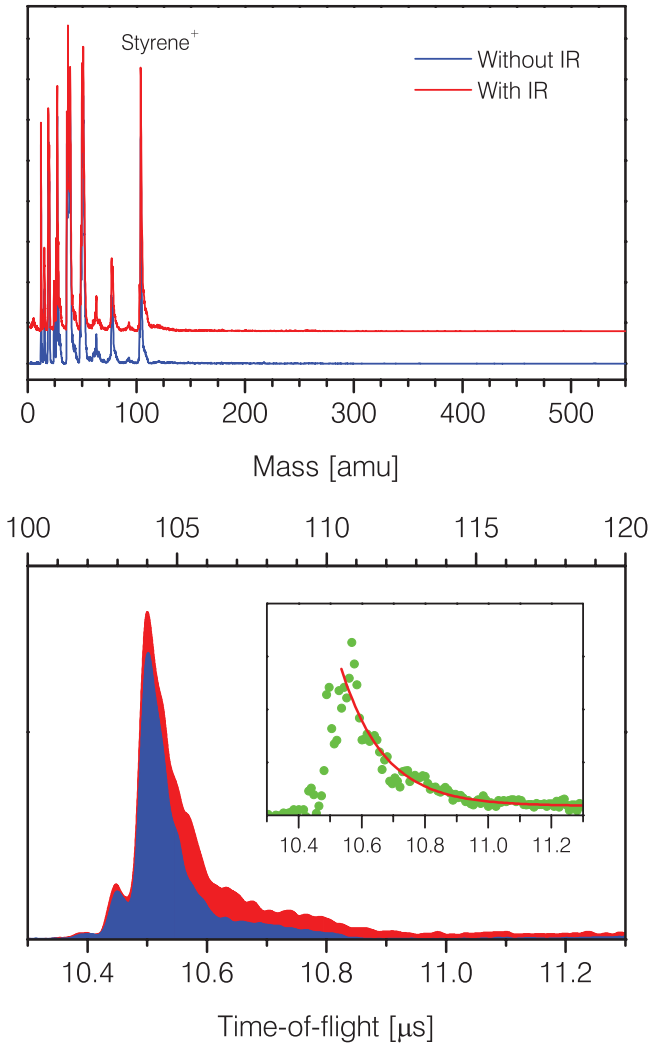

FIG. 8. (Upper panel) Time-of-flight mass spectra in the absence and presence of IR radiation resonant with the transition at 1531 cm^{-1} of styrene cations in helium droplets. (Lower panel) Time-of-flight spectra of styrene cations in the presence and absence of resonant IR radiation. The inset shows the difference between the two time-of-flight spectra.

the ejection of the ions from the helium droplets.[10] In order to determine whether the same mechanism is operational when ions are excited at lower vibrational energies, we have recorded mass spectra and analyzed the speed distributions of the desolvated ions. The upper panel of Fig. 8 shows two time-of-flight mass spectra recorded following the non-resonant ionization of styrene molecules in helium droplets consisting on average of 2700 atoms before pickup of the molecules. One spectrum has been recorded in the presence of IR radiation resonant with the vibrational transition at 1531 cm^{-1}, while the other spectrum has been recorded in the absence of IR radiation. The low mass range of both spectra is dominated by ions resulting from background gas and is independent of the IR radiation. The part of the mass spectra related to the styrene molecule is characterized by a strong peak at mass 104 amu, corresponding to the styrene cation, and a much weaker peak at 103 amu, corresponding to hydrogen loss of the styrene ion. Most importantly, no evidence of IR induced formation of styrene^{+}He$_n$ complexes is observed

in the high mass range of the spectra. In our previous study, we have extensively discussed the possible different experimental outcomes for thermal and non-thermal desolvation processes.[10] It was concluded that a thermally driven evaporative process would yield large ion-containing helium clusters, while a non-thermal process would yield mainly bare ions. The absence of large styrene$^+$He$_n$ complexes in the mass spectrum is thus incompatible with the generally accepted cooling mechanism but in support of the ejection of the ions from the helium droplets. Closer inspection of the styrene cation signal reveals a small difference in the line shape of these peaks. This difference is more clearly seen in the lower panel of Fig. 8 where both signals are now compared as function of flight time. The signal recorded in the presence of the resonant IR radiation shows a noticeable tail towards longer flight times. By taking the difference between the spectra, see inset Fig. 8, one finds that the IR induced signal rises promptly and then decays almost exponentially on a time scale of 200 ns. When interpreting the time dependence of this signal the pulse structure of FELIX has to be taken into account. As mentioned before, the IR macropulse of FELIX consists of micropulses separated by 1 ns. On the time scale of the time-of-flight spectrum shown in Fig. 8 the ions are thus illuminated quasi-continuously by IR radiation. Therefore, the IR induced signal reflects the number of styrene cations produced at a given time after creation of the ions by the UV laser pulse. The prompt rise of the signal implies that styrene cations are formed instantaneous, which gives further support to the hypothesis that the ions are ejected from the droplets following vibrational excitation. Two processes are expected to contribute to the decay of the signal. First, due to the applied electric field the ion containing helium droplets remain only a limited period of time in the IR excitation region. Based on the strength of the applied electric fields, estimated droplet size and IR beam diameter at the focus, the time scale for this process is expected to be in the range of hundreds of nanoseconds. Second, the number of ion-containing helium droplets is depleted by the IR excitation of the styrene ions. Since the effect of the IR laser intensity and droplet size on the decay time has not been systematically investigated, the relative importance of both processes cannot be determined here.

Additional information on the process taking place after vibrational excitation of the ions can be obtained from the speed distributions of the ions. Figure 9 shows ion images recorded following the vibrational excitation of DPE cations at 334 and 1547 cm^{-1}. The images are very similar and show isotropic angular distributions. The speed distributions derived from these images are almost identical, even though the IR excitation frequencies differ by almost a factor of five. The speed distributions, which are found to be largely independent of helium droplet size, can be accurately fitted to Maxwell-Boltzmann distributions with translational temperatures of ~25 K. The two other systems investigated in this study, aniline and styrene, show similar characteristics, i.e., a weak dependence of the translational temperature on excitation energy and no significant dependence on droplet size. The difference between the three systems is found in the magnitude of the translational temperature of the ions. Whereas the temperature of the DPE ions is ~25 K when excited around

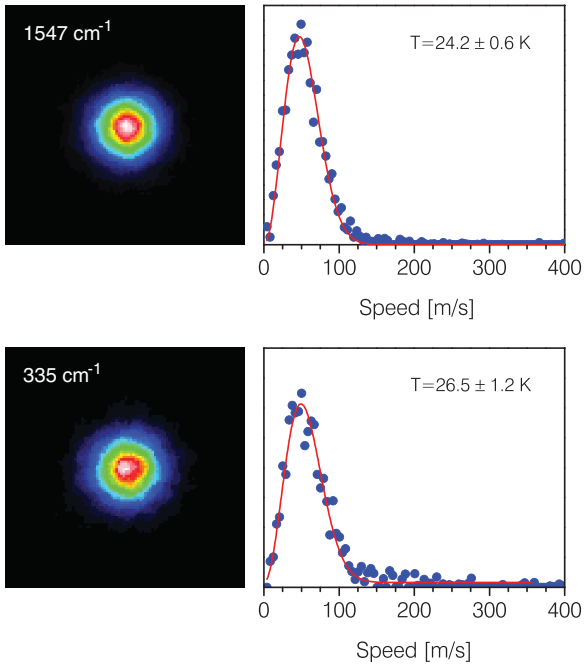

FIG. 9. Ion images and corresponding speed distribution of desolvated 1,1-diphenylethylene cations following excitation at 1547 and 335 cm^{-1}. The solid line is a fit of the data to a Maxwell-Boltzmann distribution with a temperature as indicated in the figure.

1500 cm^{-1}, that of the styrene and aniline cations are around 40 and 65 K, respectively. From this data it appears that the translational temperature of the ejected ions correlates to either the size or the mass of the ions, since the smaller and lighter cations yield higher temperatures. Unfortunately, it is not possible with the current limited data set to determine the exact relationship between these molecular properties and the kinetic energy of the ions.

While the translational temperature of the ejected ions varies strongly with the ion, it depends only weakly on the excitation energy. The translational temperatures of the ions as determined at different excitation energies are presented in Fig. 10. Included in this graph are also the temperatures

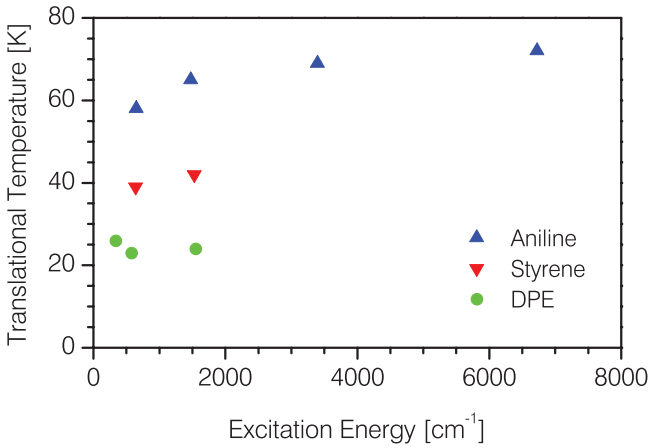

FIG. 10. Translational temperature of aniline, styrene, and 1,1-diphenylethylene (DPE) cations ejected from helium droplets as function of excitation energy. The droplets consist on average of 2700 helium atoms.

of aniline cations found in our initial study where the fundamental and overtone transitions of the NH-stretch vibration were excited at 3395 and 6725 cm^{-1}, respectively. In the case of the aniline cation, an increase of the excitation energy by more than one order of magnitude, i.e., from 659 cm^{-1} to 6725 cm^{-1}, increases the translational temperature of ions only slightly from 58 to 72 K. This variation is much smaller than the difference in temperatures found between the different ionic systems. The translational temperatures of the ejected ions correspond to a large fraction of the excitation energy. For example, the translational energy of the aniline ions after excitation via the transition at 659 cm^{-1} corresponds to 6% of the excitation energy. This is a considerable fraction of the energy in view of the large size of the helium droplet system. The substantial kinetic energy of the ions and the fact that this energy does not depend strongly on the droplet size seem to indicate that the processes leading to the ejection of the ions mainly involves the helium in the close vicinity of the ion. Although the present data set gives some indications regarding the processes leading to the ejection of the ions, we prefer not to speculate here about a possible mechanism.

IV. CONCLUSION

Vibrational spectra of aniline, styrene, and 1,1-diphenylethyl cations embedded in helium droplets have been recorded. Comparison of the spectra to their gas phase counterparts reveals that the helium environment induces an almost negligible matrix shift, analogous to what has been found for neutral molecules. The linewidths of the transitions are limited by the bandwidth of the light source and show no noticeable helium-induced broadening. In this respect helium droplets can be considered as much as an ideal spectroscopic matrix for ions as for neutrals. The recorded spectra have provided new and improved vibrational frequencies for the styrene and 1,1-diphenylethyl cations, as well as for neutral aniline and styrene. Evidence has been put forward that the desolvation of the embedded ions after excitation is governed by a non-evaporative process in which the ions are ejected from the droplets. The kinetic energy of the desolvated ions is molecule specific and depends only very weakly on the excitation energy. Although these observations provide new insight into the desolvation dynamics of excited ions in helium droplets, the current data are too limited to establish the mechanism leading to the ejection of the ions.

ACKNOWLEDGMENTS

This work was supported by the EPFL, the Swiss National Science Foundation (NSF(CH)) through Grant No. 200020-119789, and the Nederlandse Organisatie voor Wetenschappelijk Onderzoek (NWO). The research leading to these results has received funding from the European Community's Seventh Framework Programme (FP7/2007-2013) under grant agreement No. 226716. We would like to thank Professor W. J. Buma for stimulating discussions and the FELIX staff for their skilled technical assistance.

[1] J. P. Toennies and A. F. Vilesov, Angew. Chem., Int. Ed. **43**, 2622 (2004).
[2] F. Stienkemeier and A. F. Vilesov, J. Chem. Phys. **115**, 10119 (2001).
[3] K. K. Lehmann and G. Scoles, Science **279**, 2065 (1998).
[4] M. Y. Choi, G. E. Douberly, T. M. Falconer, W. K. Lewis, C. M. Lindsay, J. M. Merritt, P. L. Stiles, and R. E. Miller, Int. Rev. Phys. Chem. **25**, 15 (2006).
[5] K. Nauta and R. E. Miller, Science **283**, 1895 (1999).
[6] K. Nauta and R. E. Miller, Science **287**, 293 (2000).
[7] K. Nauta, D. T. Moore, P. L. Stiles, and R. E. Miller, Science **292**, 481 (2001).
[8] F. Dong and R. E. Miller, Science **298**, 1227 (2002).
[9] F. Bierau, P. Kupser, G. Meijer, and G. von Helden, Phys. Rev. Lett. **105**, 133402 (2010).
[10] S. Smolarek, N. B. Brauer, W. J. Buma, and M. Drabbels, J. Am. Chem. Soc. **132**, 14086 (2010).
[11] N. B. Brauer, S. Smolarek, X. H. Zhang, W. J. Buma, and M. Drabbels, J. Phys. Chem. Lett. **2**, 1563 (2011).
[12] J. M. Merritt, G. E. Douberly, and R. E. Miller, J. Chem. Phys. **121**, 1309 (2004).
[13] E. Loginov, A. Braun, and M. Drabbels, Phys. Chem. Chem. Phys. **10**, 6107 (2008).
[14] D. M. Brink and S. Stringari, Z. Phys. D: At., Mol. Clusters **15**, 257 (1990).
[15] D. Oepts, A. F. G. van der Meer, and P. W. van Amersfoort, Infrared Phys. Technol. **36**, 297 (1995).
[16] X. B. Song, M. Yang, E. R. Davidson, and J. P. Reilly, J. Chem. Phys. **99**, 3224 (1993).
[17] Z. Xu, J. M. Smith, and J. L. Knee, J. Chem. Phys. **97**, 2843 (1992).
[18] M. Takahashi, H. Ozeki, and K. Kimura, J. Chem. Phys. **96**, 6399 (1992).
[19] X. Zhang, J. M. Smith, and J. L. Knee, J. Chem. Phys. **99**, 3133 (1993).
[20] J. M. Smith and J. L. Knee, Laser Chem. **14**, 131 (1994).
[21] J. M. Dyke, H. Ozeki, M. Takahashi, M. C. R. Cockett, and K. Kimura, J. Chem. Phys. **97**, 8926 (1992).
[22] S. Smolarek, A. Vdovin, A. Rijs, C. A. van Walree, M. Z. Zgierski, and W. J. Buma, J. Phys. Chem. A **115**, 9399 (2011).
[23] C. Gee, S. Douin, C. Crepin, and P. Brechignac, Chem. Phys. Lett. **338**, 130 (2001).
[24] H. Piest, G. von Helden, and G. Meijer, J. Chem. Phys. **110**, 2010 (1999).
[25] A. Braun and M. Drabbels, J. Chem. Phys. **127**, 114303 (2007).
[26] E. Loginov and M. Drabbels, J. Phys. Chem. A **111**, 7504 (2007).
[27] M. Lewerenz, B. Schilling, and J. P. Toennies, Chem. Phys. Lett. **206**, 381 (1993).
[28] E. Loginov, D. Rossi, and M. Drabbels, Phys. Rev. Lett. **95**, 163401 (2005).
[29] P. M. Wojciechowski, W. Zierkiewicz, D. Michalska, and P. Hobza, J. Chem. Phys. **118**, 10900 (2003).
[30] T. Nakanaga and F. Ito, Chem. Phys. Lett. **355**, 109 (2002).
[31] N. Solca and O. Dopfer, Eur. Phys. J. D **20**, 469 (2002).
[32] Y. Kwon, P. Huang, M. V. Patel, D. Blume, and K. B. Whaley, J. Chem. Phys. **113**, 6469 (2000).
[33] A. Nakayama and K. Yamashita, J. Chem. Phys. **112**, 10966 (2000).
[34] C. Di Paola, F. Sebastianelli, E. Bodo, I. Baccarelli, F. A. Gianturco, and M. Yurtsever, J. Chem. Theory Comput. **1**, 1045 (2005).
[35] J. C. Evans, Spectrochim. Acta **16**, 428 (1960).
[36] A. Uskola, F. J. Basterretxea, and F. Castano, J. Mol. Struct. **609**, 187 (2002).
[37] See supplementary material at http://dx.doi.org/10.1063/1.3678011 for a listing of the calculated vibrational frequencies of styrene and DPE cation and a description of the ion-dip double-resonance spectroscopy experiment on neutral aniline.
[38] M. Lewerenz, B. Schilling, and J. P. Toennies, J. Chem. Phys. **102**, 8191 (1995).
[39] D. van Heijnsbergen, G. von Helden, G. Meijer, P. Maitre, and M. A. Duncan, J. Am. Chem. Soc. **124**, 1562 (2002).
[40] T. Nakanaga, P. K. Chowdhury, F. Ito, K. Sugawara, and H. Takeo, J. Mol. Struct. **413**, 205 (1997).
[41] N. Yamamoto, K. Ohashi, K. Hino, H. Izutsu, K. Mogi, Y. Sakai, and H. Sekiya, Chem. Phys. Lett. **345**, 532 (2001).
[42] K. Ohashi, Y. Inokuchi, H. Izutsu, K. Hino, N. Yamamoto, N. Nishi, and H. Sekiya, Chem. Phys. Lett. **323**, 43 (2000).
[43] M. J. Frisch, G. W. Trucks, H. B. Schlegel *et al.*, GAUSSIAN 09, Revision A.02, Gaussian, Inc., Wallingford, CT, 2009.
[44] F. Madeja, M. Havenith, K. Nauta, R. E. Miller, J. Chocholousova, and P. Hobza, J. Chem. Phys. **120**, 10554 (2004).

[45]M. Schutz and D. Schemmel, J. Chem. Phys. **132**, 174303 (2010).
[46]N. Yamamoto, K. Hino, K. Mogi, K. Ohashi, Y. Sakai, and H. Sekiya, Chem. Phys. Lett. **342**, 417 (2001).
[47]E. B. Wilson, Phys. Rev. **45**, 0706 (1934).
[48]I. Baraldi, E. Gallinella, and M. Scoponi, Spectrochim. Acta, Part A **43**, 1045 (1987).
[49]M. Hartmann, A. Lindinger, J. P. Toennies, and A. F. Vilesov, J. Phys. Chem. A **105**, 6369 (2001).
[50]R. Lehnig and A. Slenczka, J. Chem. Phys. **118**, 8256 (2003).
[51]P. Radcliffe, A. Przystawik, T. Diederich, T. Doppner, J. Tiggesbaumker, and K. H. Meiwes-Broer, Phys. Rev. Lett. **92**, 173403 (2004).
[52]A. Marchand and J. P. Quintard, Spectrochim. Acta, Part A **36**, 941 (1980).